

Cite this: DOI: 10.1039/c1jm00063b

www.rsc.org/materials

PAPER

## Modification of the refractive-index contrast in polymer opal films†

P. Spahn,<sup>\*a</sup> C. E. Finlayson,<sup>‡\*b</sup> W. Mbi Etah,<sup>a</sup> D. R. E. Snoswell,<sup>b</sup> J. J. Baumberg<sup>\*b</sup> and G. P. Hellmann<sup>a</sup>

Received 5th January 2011, Accepted 15th April 2011

DOI: 10.1039/c1jm00063b

Synthetic opals, based on self-assembled arrays of core-shell (bead/matrix) polymer microspheres, are a promising platform for next-generation photonic structures, coatings and sensors. The refractive index contrast ( $\Delta n$ ) between beads and the matrix polymer is essential for the appearance of structural colour in polymer opal films. We report how the index contrast can be modified by engineering the chemical composition of the core-interlayer-shell (CIS) precursor particles. Alternative approaches to emulsion polymerisation, using the fluorinated monomer 2,2,2-trifluoroethyl acrylate and the aromatic monomer benzyl acrylate, yield a much larger range of  $\Delta n$  values than for standard systems made from styrene and ethyl acrylate. Spectroscopic studies reveal striking differences in the transmission properties of thin-films as  $\Delta n$  is varied from 0.045 up to 0.18.

## Introduction

A cost-effective, large-scale technique to produce flexible opals through melting and shear-ordering under compression, utilizing a core/shell approach based on polymers, has recently been developed.<sup>1–6</sup> These polymeric opal systems are based on ensembles of core-interlayer-shell (CIS) particles, synthesized by an emulsion polymerisation process. The high-quality low-defect single-domain flexible polymer opals possess fundamental optical resonances tuneable across the visible and near-infrared regions, by varying the precursor nano-sphere size (from 200–350 nm) and hence the resulting *fcc* lattice parameter. Contrary to reflective iridescence based on Bragg diffraction, in the low refractive-index contrast regime associated with these polymer composites, colour generation arises through spectrally resonant scattering inside a 3D *fcc*-lattice photonic crystal,<sup>7,8</sup> in a similar fashion to the iridescence in natural opals.<sup>9</sup> In addition, one of the most attractive features of elastomeric polymer opals is the tunability of their perceived colour by the bending or stretch modification of the (111) plane spacing. However, the refractive index contrast between the core beads and the matrix polymer is essential for the appearance of structural colour in polymer opal films.

In our earlier work,<sup>1,2,10,11</sup> we reported the synthesis of rigid cross-linked polystyrene (PS) spheres, capped by a soft polyethyl acrylate (PEA) shell *via* a grafting layer (see Fig. 1)

containing the asymmetrical, difunctional allyl methacrylate (ALMA) as a co-monomer. The net refractive index contrast between core and shell material is  $\Delta n \approx 0.11$ . In this paper, we report a significant advance from the archetypal PS-PEA structure, in that the index contrast can be varied by engineering the chemical composition of the CIS precursor particles. Alternative approaches, using the fluorinated monomer 2,2,2-trifluoroethyl acrylate (TFEA) and the aromatic monomer benzyl acrylate (BzA), enable us to prepare samples with  $\Delta n$  in the range from 0.045 up to 0.18. The primary motivation for this work being to maximise the structural colour effects in polymer opal thin-films. Spectroscopic studies reveal very significant differences in the optical properties of processed opaline thin-films, as a function of  $\Delta n$ . All samples exhibit optical resonances in the visible part of the spectrum, and the optical density associated with these resonances is seen to increase very strongly with increasing index-contrast.

The synthesis (described below) uses semicontinuous, step-wise emulsion polymerisation for the controlled build-up of the CIS particle architecture. The formation of core-shell structures in emulsion polymerisation is generally governed by hydrophilicity and interface energies.<sup>12–14</sup> Because of the outstanding

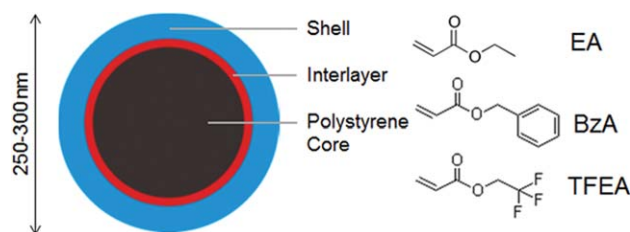


Fig. 1 (left) Core-interlayer-shell (CIS) particle architecture, drawn to relative scale. (right) The chemical structures of the precursor monomers for the shell, EA, BzA and TFEA.

<sup>a</sup>Deutsches Kunststoff-Institut, Schlossgartenstrasse 6, D-64289 Darmstadt, Germany. E-mail: PSpahn@dki.tu-darmstadt.de; Fax: +49 6151 292855; Tel: +49 6151 162104

<sup>b</sup>NanoPhotonics Centre, University of Cambridge, Cambridge, CB3 0HE, UK. E-mail: jjb12@cam.ac.uk; Fax: +44 (0)1223 764515; Tel: +44 (0) 1223 761671

† Electronic supplementary information (ESI) available. See DOI: 10.1039/c1jm00063b

‡ Current address: Institute of Mathematical and Physical Sciences, Aberystwyth University, Wales SY23 3BZ, UK. E-mail: cef2@aber.ac.uk

hydrophobicity and low water-solubility of fluorinated monomers, earlier work used methyl- $\beta$ -cyclodextrin as a phase transfer catalyst to enhance the solubility, and a copolymerisation approach to increase the compatibility of core and shell polymers.<sup>15</sup> Other works succeeded in the synthesis of particles with fluorinated monomers (homogeneous or core-shell), suitable for the formation of colloidal crystals without these auxiliaries, using surfactant-free emulsion polymerisation.<sup>16,17</sup>

The surfactant-free emulsion polymerisation is commonly considered as being the appropriate means to yield the monodisperse particle size distribution necessary for the formation of high-quality colloidal crystals, although we have found that surfactants can be used under strictly controlled conditions without impairing the particle size distribution. It is mandatory to add the monomer dropwise, thus avoiding any enrichment of monomers droplets or surfactants in the aqueous phase (starved-feed conditions). The use of surfactants renders the synthesis more robust to variations of the reaction conditions and thus enables the facile adjustment of the chemical composition.<sup>18</sup> All samples described in this paper contain 3% of hydroxyethyl methacrylate as a co-monomer in the shell polymer.

## Results and discussion

### 1. Synthesis and characterisation of the homopolymers§

A 250 mL round bottom flask with a mixture of 100 g of demineralised water (saturated with inert gas), 0.05 g of dodecyl sulfate and 10 g of trifluoroethyl acrylate or benzyl acrylate was heated at 75 °C under magnetic stirring. A solution of 0.2 g of sodium persulfate in 5 mL of demineralised water was added and the stirring was continued for two hours. A white latex was observed to form and the product was filtered through a 100  $\mu$ m sieve. The pure polymer was collected by the evaporation of the water in a convective oven set to 45 °C.

The polymerisation of trifluoroethyl acrylate and benzyl acrylate was successful, although a significant amount (1.5 g) of precipitate formed during the polymerisation of the trifluoroethyl acrylate at the glass wall of the flask. The homopolymers were soft and sticky solids. They have been further characterised by differential scanning calorimetry (DSC) and thermal gravimetric analysis (TGA) (see ESI†, Fig. S1).

DSC was used to estimate the glass transition temperatures ( $T_g$ ). The glass transition temperatures of polybenzyl acrylate  $T_g$  (PBzA) = +12 °C and polytrifluoroethyl acrylate  $T_g$  (TFEA) = +2 °C are higher than the glass transition temperature of polyethyl acrylate  $T_g$  (PEA) = -15 °C, but still significantly below room temperature. As the processing of the opal polymers takes place at temperatures of about 120–150 °C, BzA and TFEA were considered as a good choice to replace the

EA, without critically changing the mechanical and rheological properties of the shell polymer and the viscoelastic melt. TGA was used to check if polymer decomposition was significant at the temperatures (<200 °C) used for polymer processing. A significant decomposition of the polybenzyl acrylate does occur at >250 °C and the polytrifluoroethyl acrylate starts to decompose at >300 °C. Both were considered as sufficiently stable for the subsequent processing with extruder and press. Whilst the successful syntheses of the homopolymers showed that trifluoroethyl acrylate and benzyl acrylate are suitable for emulsion polymerisation, they gave no indication whether these monomers form smooth shells onto polystyrene cores. Such shape integrity is critical for the assembly of the CIS particles into ordered lattice arrays, giving opaline properties.

### 2. Synthesis and processing of CIS-particles§

The syntheses with benzyl acrylate and trifluoroethyl acrylate were conducted in a 1 L glass reactor equipped with condenser, mechanical stirrer and inert gas inlet (Fig. S2†). The CIS-particles consist of a polystyrene core, crosslinked with 10 wt% of butanediol diacrylate (BDDA), an interlayer of a copolymer with the grafting agent allyl methacrylate (ALMA) and a shell of mostly grafted, but linear polymer chains. The ratio of the monomers used for the polymerisation was core : interlayer : shell = 31.4 : 11.4 : 57.2 by weight (Fig. 1). The monomers were emulsified with dodecyl sulfate and the commercial surfactant Dowfax 2A1 (alkyldiphenyloxide disulfonate salt) in water prior to the addition. All monomer emulsions were added dropwise into the reactor *via* a precise piston pump strictly maintaining starved-feed conditions. The polymerisation of both the core and the shell polymers was initiated by a one-shot addition of sodium persulfate (see ESI† for detailed description).

The batches differ in the polymer composition of the interlayer and the shell, as given in overview in Table 1. The beads of sample 3 (made earlier in a 10 L scale) have a shell made from ethyl acrylate (EA) and an interlayer made from ethyl acrylate and the grafting agent allyl methacrylate (10 wt%). This system is identical to that previously reported, with  $\Delta n \approx 0.11$ .<sup>1–4</sup> Samples 1 and 2 are examples with enhanced refractive index contrast, as the shell layer contains the fluorinated monomer TFEA, which decreases the refractive index of the shell polymer. Samples 4 and 5 are examples with impaired refractive index contrast, as the shell of these beads is a copolymer of benzyl acrylate (BzA) and ethyl acrylate, with the BzA increasing the net refractive index of the shell polymer. The interlayer always consisted of the same monomers as the shell polymer, plus 10 wt% of the grafting agent ALMA. The shell polymer of each sample contains a negligible amount of 3 wt% of hydroxyethyl methacrylate (HEMA) as a comonomer to enable later crosslinking.

We observed that the polymerisation of the copolymers with BzA and especially with the TFEA was significantly slower than the polymerisation of the pure EA. The monomer emulsions with TFEA required vigorous stirring to prevent phase separation and a careful control of the addition rate to maintain the starved-feed conditions. The aqueous lattices were then coagulated in methanol with an addition of sodium chloride. The precipitate was washed once with demineralised water, filtered off and dried in a convective oven at 45 °C for three days. The chunks of dried

§ Chemicals: the monomers styrene and ethyl acrylate (BASF SE), benzyl acrylate (Osaka Chem.) and 2,2,2-trifluoroethyl acrylate (Fluorochem Ltd.) have been distilled under reduced pressure prior to use. Butanediol diacrylate (BASF SE) and allyl methacrylate (Evonik Industries AG) have been passed over an ion exchange column (Dehibit 200, PolymerScience) for the removal of the inhibitor. Dowfax 2A1 (The Dow Chemical Company) was provided by Nordmann, Rassmann GmbH. Dowfax and all other chemicals (Sigma Aldrich) were used as provided. The demineralised water was saturated with nitrogen prior to use.

**Table 1** Detailed polymer composition of samples under study

Sample	Core	Interlayer	Shell
1	Styrene : BDDA = 90 : 10	EA : TFEA : ALMA = 0 : 90 : 10	EA : TFEA : HEMA = 0 : 97 : 3
2	Styrene : BDDA = 90 : 10	EA : TFEA : ALMA = 45 : 45 : 10	EA : TFEA : HEMA = 48.5 : 48.5 : 3
3	Styrene : BDDA = 90 : 10	EA : ALMA = 90 : 10	EA : HEMA = 97 : 3
4	Styrene : BDDA = 90 : 10	EA : BzA : ALMA = 45 : 45 : 10	EA : BzA : HEMA = 48.5 : 48.5 : 3
5	Styrene : BDDA = 90 : 10	EA : BzA : ALMA = 22.5 : 67.5 : 10	EA : BzA : HEMA = 24.25 : 72.75 : 3

polymer were cut manually and extruded to obtain a homogeneous strand: 10 g of each polymer were extruded in the flush mode of the *DSM xplora μ5* micro-extruder, operated at a temperature of 140 °C and with a counter-rotating screw speed of 86 rpm. The strands made from sample 2 and especially from sample 1 were significantly less elastic than the reference polymer of sample 3.

Opaline disks were then made by processing the polymer strands with a *Dr Collin* hydraulic press. 5 g of polymer strand was coiled up and heated on a hotplate set to 130 °C until softened. The mass was further compacted with a spatula and then pressed between PET foils and glossy steel plates at 150 °C and 170 bar hydraulic pressure for 3 minutes. Samples 3, 4 and 5 formed uniform disks with a smooth surface, 150–250 μm thick. The opal disks made from 3 and 4 visually showed strong structural colour, whilst the colour of the disk made from 5 (lowest  $\Delta n$ ) was significantly weaker. For the batches of samples 1 and 2 (with the fluorinated monomers) the manufacturing of the opal films turned out to be less straight-forward. The flow of the melt was rather less even and uniform, probably due to the low surface tension of the fluorinated polymers. Thinner films turned out to behave better, with smooth opal films being made by pressing a reduced amount (2–2.5 g) of the extruded strands. The higher pressure (smaller sample area) yielded a lower film thickness of 120–150 μm. Overall, a careful control of the temperature of processing and film thickness was needed to achieve opaline films of a satisfactory quality. We note that the high processing temperature of 150 °C will likely mean that no strain is built into the system and that the soft shells are therefore compliant with the cubic packing order of the spheres. In recent work the ordering in thin-films of polymeric opals was observed to undergo a remarkable improvement by using an edge-shearing technique to give enhanced structural colour effects.<sup>19</sup> In this present work, strips of the opal disks were processed manually over a hot edge heated to 120 °C, before the measurement of UV/vis spectra in transmission.

The quality of the CIS particles was examined with transmission electron microscopy (TEM) and with hydrodynamic chromatography (PL-PSDA, Varian Inc.). TEM suffers from a drawback that the soft shell polymers flow under the influence of the electron beam. Therefore, the amount of particle impurities cannot be reasonably estimated with TEM images because of film formation. However, the smooth particle surfaces and the spherical shape shown in the TEM images of Fig. 2 indicate that the use of trifluoroethyl acrylate and benzyl acrylate did not lead to incomplete formation of the shells. The particle size distribution was measured with the PL-PSDA and Table 2 gives the coefficient of variation (CoV) for the measured particle size distributions. Our experience is that a coefficient <0.12 is sufficient for opal films of optimal quality. The coefficients for the

particle size distribution of the reference batch sample 3 and for samples 4 and 5 with BzA are excellent, whereas the samples 1 and 2 with TFEA are slightly worse, but still give films with a strikingly intense structural colour effect.

A closer inspection of the particle size distributions given in Fig. 3 reveals that the difference is due to large particle impurities in the batches with trifluoroethyl acrylate. The width of the particle size distribution of the main fraction is similar to the particle size distribution of the batches without trifluoroethyl acrylate (Fig. 3a). Although small in concentration, the huge particle size of the impurities (Fig. 3b) has a dramatic effect on the coefficient of variation. As the PS cores have been made in the same way for all batches, the aggregates must be due to the trifluoroethyl acrylate and they must form during or after the synthesis of the interlayer and the shell. This presumption is supported by the observation that the aggregates have about twice the size of the main fraction which indicates the formation of dimers. It is reasonable to suggest that, in future work, the impurities might be eliminated by variation of the emulsion polymerisation, with the type and concentration of the surfactants and the rate of the monomer addition being optimized.

As described earlier, the purpose of using trifluoroethyl acrylate and benzyl acrylate was to alter the refractive index of the PEA shell polymer. The numbers for the refractive index contrast in Table 2 were calculated from literature values of the refractive indices of the homopolymers ( $n(\text{PBzA}) = 1.55$ ;  $n(\text{PTFEA}) = 1.407$ ), the indices of  $n(\text{PS}) = 1.58$ ,  $n(\text{PEA}) = 1.47$ , and the volume fractions of the monomers in the copolymers. Additionally, as a check for consistency, the average refractive-indices ( $n_{\text{av}}$ ) were measured using a standard Abbe refractometer instrument.

### 3. Optical spectroscopy

A dependency of the structural colour of the opal films on the refractive index contrast was clearly visible. Most appealing is

**Table 2** Characteristic parameters for all samples: measured average refractive-index,<sup>a</sup> calculated index-contrast, co-efficient of variation in particle size (CoV),<sup>b</sup> particle size, normal incidence Bragg wavelength ( $\lambda_{111}$ ) and fitted FWHM

Sample	$n_{\text{av}}$	$\Delta n$	CoV	CIS size/nm	$\lambda_{111}$ /nm	FWHM/nm
1	1.488	0.18	0.217	270	595	44.0
2	1.505	0.15	0.196	285	580	46.5
3	1.517	0.12	0.079	280	605	87.0
4	1.548	0.07	0.070	275	625	92.4
5	1.565	0.045	0.071	255	680	>100

<sup>a</sup> The measured Abbe refractometer angles were 18°55', 20°15', 22°5', 25°40' and 27°50' for samples 1–5, respectively. <sup>b</sup> CoV is defined as the ratio of standard deviation to the mean value.

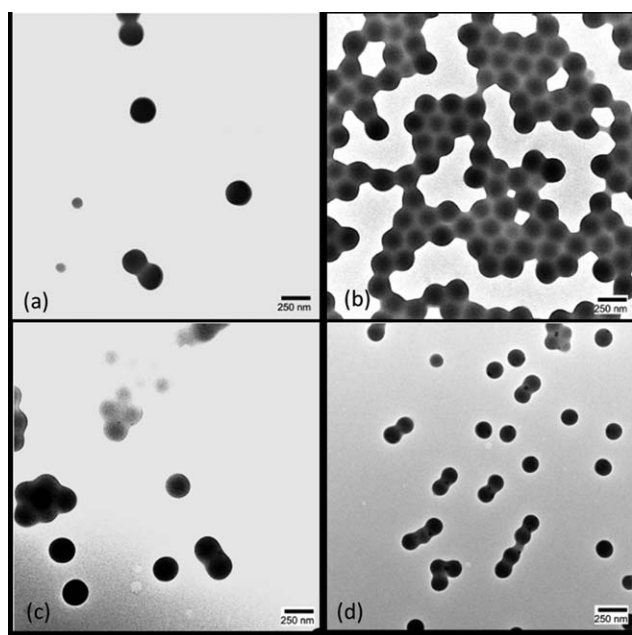


**Fig. 2** TEM images of dried particles: (a) sample 1, (b) sample 2, (c) sample 4, and (d) sample 5.

the huge difference in the intensity of the transmitted colours which is apparent in Fig. 4 (inset); the effect is obvious even to the naked eye.

It was possible to measure the differences in the optical transmission spectra with the *Perkin Elmer Lambda 40* spectrometer. The spectra in Fig. 4 do not have the very high quality which we previously observed from <100  $\mu\text{m}$  thin films processed over the hot edge,<sup>19</sup> nevertheless, well defined opaline resonances are in evidence for all of the samples and huge differences in the scattering intensity are apparent. To a first approximation,<sup>20</sup> it is expected that the Bragg wavelength ( $\lambda_{111}$ ) will vary as a function of the CIS mean particle diameter ( $d$ ) and the average refractive-index ( $n_{\text{av}}$ ) according to eqn (1).

$$\lambda_{111} \approx \sqrt{(3/2)dn_{\text{av}}} \quad (1)$$

Hence, the variation of  $\lambda_{111}$  between samples is not due to the changes in  $\Delta n$ , but rather due to variations in the exact CIS mean

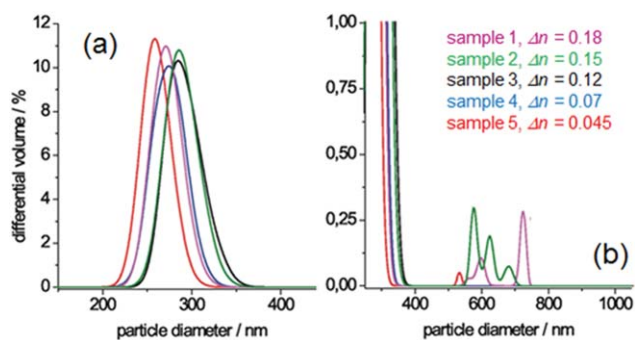


**Fig. 3** Particle size distribution determined with hydrodynamic chromatography (PL-PSDA, Varian Inc.) in the range of (a) 150–450 nm and (b) 400–1000 nm.

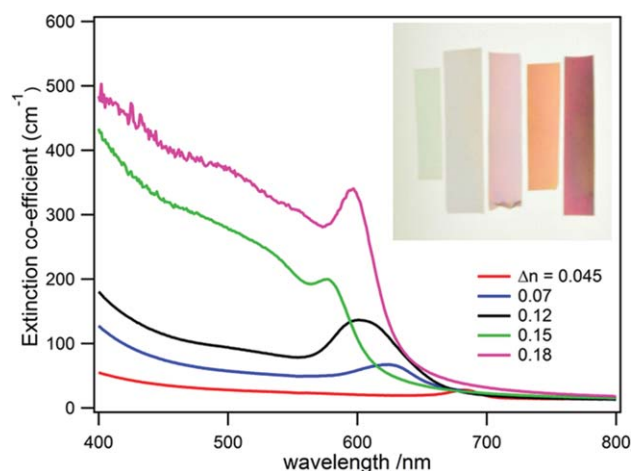


**Fig. 4** UV/vis spectra of hot-edge processed pieces of thin opal disks with different refractive index contrasts. The samples have a similar thickness of 130–140  $\mu\text{m}$  and have been normalised to give the intensive units of extinction co-efficient. The inset shows the samples as viewed in transmitted light, with the index contrast increasing from left to right.

particle size, as summarised in Table 2. The samples with lower  $\Delta n$  are also generally characterised by a red-shifted absorbance, due to the higher average refractive index. Whilst we attempted to produce opals with a Bragg peak in the red region of the spectrum each time, there was evidently some variation between around 580–680 nm in the final samples.

The increase in absorbance intensity corresponds neatly with the increase in refractive index contrast, with the change of the visual impression of the intensity of the transmission colour with increasing refractive index contrast also matching the measured increase of absorbance in the UV/vis spectra. As a further measure of the improvement in the resonant structural colour effect, the Bragg peaks in Fig. 4 were fitted to Lorentzian line profiles (see ESI†, Fig. S3) and the full-width half-maximum values extracted, as shown in Table 2. There is a reasonably clear trend for the FWHM values to decrease with increasing  $\Delta n$ , as the “sharpness” of the observed resonance improves.

The change of the transmitted colour intensity with relatively small variations of the refractive index contrast is very marked. Currently these effects, which have not been reported previously, are not well understood and a future paper will describe the theoretical modelling of such behaviour. These results are very encouraging and promising from the perspective of being able to extend the paradigm of the CIS opaline system into a wider range of engineered functionalities and a wider array of applications. In particular, the availability of polymeric opal samples with different index contrasts will allow more detailed studies of many interesting physical phenomena of these systems, such as the role of structural scattering and interference effects, optical band gap,<sup>21</sup> and the “scattering cone”.<sup>7</sup>

## Conclusions

In this paper, we report a significant advance in the synthesis and preparation of polymeric opal films, in that the refractive index contrast can be varied by engineering the chemical composition of the CIS composite precursor particles. Alternative approaches to emulsion polymerisation, using the fluorinated monomer

2,2,2-trifluoroethyl acrylate (TFEA) and the aromatic monomer benzyl acrylate (BzA), enable us to prepare samples with  $\Delta n$  in the range from 0.045 up to 0.18. Our approach also offers an alternative strategy for controlling refractive-index contrast, to those reported in monolithic systems, such as liquid-crystal infiltration of inverse opals.<sup>22</sup> The post-processing of particles into opaline films was demonstrated, by maintaining a careful control of the temperature of processing and film thickness in order to achieve films of a satisfactory optical quality.

Spectroscopic studies reveal very significant differences in the optical properties of opaline thin-films, as a function of  $\Delta n$ , with the optical density associated with optical resonances increasing very strongly with increasing index-contrast. The change of the transmitted colour with relatively small variations of the refractive index contrast is very marked. This engineering of the CIS structure to produce enhanced index contrast is hence likely to be of great use in improving and optimising the attractive optical properties of polymeric opals, with a wide range of potential applications,<sup>3–8</sup> spanning from photonic metamaterials and sensors, to stretchable fabrics<sup>23</sup> and decorative coatings.<sup>19</sup>

The novel use of soft nanomaterials in the design of photonic structures, with macroscale bulk-ordering, presents opportunities for a step-change away from the monolithic architectures which are currently relied upon. Our results are strongly indicative of the possibilities of extending the archetypal CIS polymer opal system, based on polystyrene/polyacrylates, into a wider range of engineered functionalities and applications.

## Acknowledgements

This work was supported by EPSRC (UK) grants EP/G060649/1 and EP/E040241.

## References

- 1 T. Ruhl, P. Spahn and G. P. Hellmann, *Polymer*, 2003, **44**, 7625–7634.
- 2 B. Viel, T. Ruhl and G. P. Hellmann, *Chem. Mater.*, 2007, **19**, 5673–5679.
- 3 O. L. J. Pursiainen, J. J. Baumberg, H. Winkler, B. Viel and T. Ruhl, *Appl. Phys. Lett.*, 2005, **87**, 101902.
- 4 O. L. J. Pursiainen, J. J. Baumberg, H. Winkler, B. Viel, P. Spahn and T. Ruhl, *Adv. Mater.*, 2008, **20**, 1484–1487.
- 5 D. R. E. Snoswell, A. Kontogeorgos, J. J. Baumberg, T. D. Lord, M. R. Mackley, P. Spahn and G. P. Hellmann, *Phys. Rev. E: Stat., Nonlinear, Soft Matter Phys.*, 2010, **81**, 020401.
- 6 A. Kontogeorgos, D. R. E. Snoswell, C. E. Finlayson, J. J. Baumberg, P. Spahn and G. P. Hellmann, *Phys. Rev. Lett.*, 2010, **105**, 233909.
- 7 O. L. J. Pursiainen, J. J. Baumberg, H. Winkler, B. Viel, P. Spahn and T. Ruhl, *Opt. Express*, 2007, **15**, 9553–9561.
- 8 J. J. Baumberg, O. L. Pursiainen and P. Spahn, *Phys. Rev. B: Condens. Matter Mater. Phys.*, 2009, **80**, 201103.
- 9 P. Vukusic and J. R. Sambles, *Nature*, 2003, **424**, 852–855.
- 10 T. Ruhl and G. P. Hellmann, *Macromol. Chem. Phys.*, 2001, **202**, 3502–3505.
- 11 T. Ruhl, P. Spahn, H. Winkler and G. P. Hellmann, *Macromol. Chem. Phys.*, 2004, **205**, 1385–1393.
- 12 Y.-C. Chen, V. Dimonie and M. S. El-Aasser, *Pure Appl. Chem.*, 1992, **64**, 1691–1696.
- 13 D. C. Sundberg and Y. G. Durant, *Polym. React. Eng.*, 2003, **11**, 379–432.
- 14 V. Herrera, R. Pirri, J. R. Leiza and J. M. Asua, *Macromolecules*, 2006, **39**, 6969–6974.
- 15 A. Alteheld, I. Gourevich, L. M. Field, C. Paquet and E. Kumacheva, *Macromolecules*, 2005, **38**, 3301–3306.
- 16 M. Egen, L. Braun, R. Zentel, K. Tannert, P. Frese, O. Reis and M. Wulf, *Macromol. Mater. Eng.*, 2004, **289**, 158–163.
- 17 I. Gourevich, L. M. Field, Z. Wei, C. Paquet, A. Petukhova, A. Alteheld, E. Kumacheva, J. J. Saarinen and J. E. Sipe, *Macromolecules*, 2006, **39**, 1449–1454.
- 18 T. Ruhl, P. Spahn, H. Winkler and G. P. Hellmann, *Prog. Colloid Polym. Sci.*, 2004, **129**, 82–87.
- 19 C. E. Finlayson, P. Spahn, D. R. E. Snoswell, G. Yates, A. Kontogeorgos, A. I. Haines, G. P. Hellmann and J. J. Baumberg, *Adv. Mater.*, 2011, **23**, 1540–1544.
- 20 S. Kim, Y. G. Seo, Y. Cho, J. Shin, S. C. Gil and W. Lee, *Bull. Korean Chem. Soc.*, 2010, **7**, 1891–1896.
- 21 R. Hillebrand, C. Jamois, J. Schilling, R. B. Wehrspohn and W. Hergert, *Phys. Status Solidi B*, 2003, **240**, 124–133.
- 22 S. Kubo, Z.-Z. Gu, K. Takahashi, A. Fujishima, H. Segawa and O. Sato, *J. Am. Chem. Soc.*, 2004, **126**, 8314–8319.
- 23 C. E. Finlayson, C. Goddard, E. Papachristodoulou, D. R. E. Snoswell, A. Kontogeorgos, P. Spahn, G. P. Hellmann, O. Hess and J. J. Baumberg, *Opt. Express*, 2011, **19**, 3144–3154.